AD-A157 930 BEHAVIOR OF IONIZED PLASMA IN THE HIGH LATITUDE TOPSIDE IONOSPHERE(U) NAVAL RESEARCH LAB WASHINGTON DC S G GANGULI ET AL. 27 AUG 85 NRL-MR-5623 1/1

UNCLASSIFIED F/G 4/1 NL

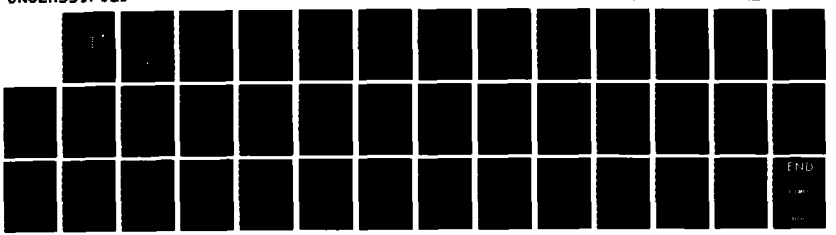

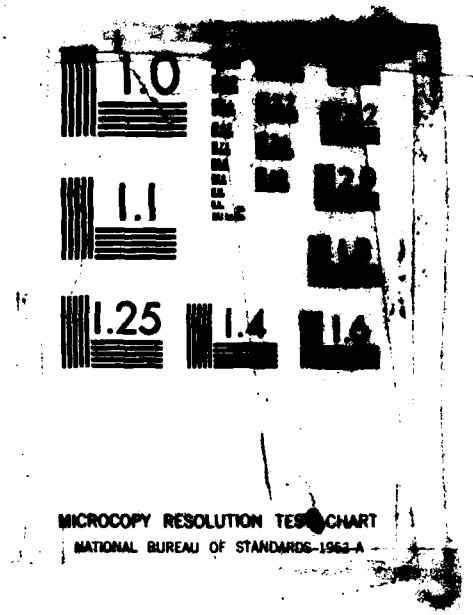
1.0
1.1
1.25
1.4
MICROCOPY RESOLUTION TEST CHART
NATIONAL BUREAU OF STANDARDS-1963-A

NRL Memorandum Report 5623

Behavior of Ionized Plasma in the High Latitude Topside Ionosphere

S. B. GANGULI AND H. G. MITCHELL, JR.

Science Applications International Corporation
McLean, VA 22102

P. J. PALMADESSO

Geophysical and Plasma Dynamics Branch
Plasma Physics Division

August 27, 1985

This work was supported by the Office of Naval Research and the National Aeronautics and Space Administration.

NAVAL RESEARCH LABORATORY
Washington, D.C.

SECURITY CLASSIFICATION OF THIS PAGE

REPORT DOCUMENTATION PAGE

1a. REPORT SECURITY CLASSIFICATION UNCLASSIFIED	1b. RESTRICTIVE MARKINGS
2a. SECURITY CLASSIFICATION AUTHORITY	3 DISTRIBUTION / AVAILABILITY OF REPORT
2b DECLASSIFICATION / DOWNGRADING SCHEDULE	Approved for public release; distribution unlimited.
4 PERFORMING ORGANIZATION REPORT NUMBER(S) NRL Memorandum Report 5623	5. MONITORING ORGANIZATION REPORT NUMBER(S)
6a NAME OF PERFORMING ORGANIZATION Naval Research Laboratory 6b OFFICE SYMBOL (If applicable) Code 4780	7a. NAME OF MONITORING ORGANIZATION
6c. ADDRESS (City, State, and ZIP Code) Washington, DC 20375-5000	7b. ADDRESS (City, State, and ZIP Code)
8a. NAME OF FUNDING / SPONSORING ORGANIZATION NASA and ONR 8b. OFFICE SYMBOL (If applicable)	9. PROCUREMENT INSTRUMENT IDENTIFICATION NUMBER
8c. ADDRESS (City, State, and ZIP Code) Washington, DC 20546 Arlington, VA 22203	10. SOURCE OF FUNDING NUMBERS PROGRAM ELEMENT NO. 61153N; PROJECT NO. W-15494; TASK NO. RR033-02-44; WORK UNIT ACCESSION NO. (See page ii)

11 TITLE (Include Security Classification)
Behavior of Ionized Plasma in the High Latitude Topside Ionosphere

12 PERSONAL AUTHOR(S)
Ganguli, S.B.,* Mitchell, H.G., Jr.* and Palmadesso, P.J.

13a. TYPE OF REPORT	13b. TIME COVERED	14. DATE OF REPORT (Year, Month, Day)	15. PAGE COUNT
Interim	FROM _____ TO _____	1985 August 27	40

16. SUPPLEMENTARY NOTATION
*Science Applications International Corporation, McLean, VA 22102 (Continues)

17 COSATI CODES		
FIELD	GROUP	SUB-GROUP

18. SUBJECT TERMS (Continue on reverse if necessary and identify by block number)
Polar wind, Adiabatic cooling, Temperature anisotropy,

19. ABSTRACT (Continue on reverse if necessary and identify by block number)

We have developed a numerical model to study the steady state behavior of a fully ionized plasma (H^+, O^+ and the electrons) encompassing the geomagnetic field lines. The theoretical formulation is based on the 16-moment system of transport equations. The electron gas is collision dominated below 2500 km. Above this altitude electron temperature anisotropy develops with temperature perpendicular to the field line being higher than that parallel to the field line. The H^+ ion temperature anisotropy shows H^+ temperature parallel to the field line being higher than that perpendicular to the field line. H^+ ion temperature also exhibits adiabatic cooling as the supersonic ion gas cools down as it expands in a diverging magnetic field. Our results are in good agreement with the previous theoretical studies of the polar wind and recent experimental observations. This is the first successful steady state solution to the 16-moment set of transport equations.

20 DISTRIBUTION / AVAILABILITY OF ABSTRACT ☒ UNCLASSIFIED/UNLIMITED ☐ SAME AS RPT ☐ DTIC USERS	21. ABSTRACT SECURITY CLASSIFICATION UNCLASSIFIED
22a NAME OF RESPONSIBLE INDIVIDUAL P. J. Palmadesso	22b. TELEPHONE (Include Area Code) (202) 767-6780 22c. OFFICE SYMBOL Code 4700.1P

DD FORM 1473, 84 MAR 83 APR edition may be used until exhausted.
All other editions are obsolete.

SECURITY CLASSIFICATION OF THIS PAGE

10. SOURCE OF FUNDING NUMBERS (Continued)

PROGRAM ELEMENT NO.	PROJECT NO.	TASK NO.	WORK UNIT ACCESSION NO.
			DN380-475 DN430-607

16. SUPPLEMENTARY NOTATION (Continued)

This work was supported by the Office of Naval Research and the National Aeronautics and Space Administration.

CONTENTS

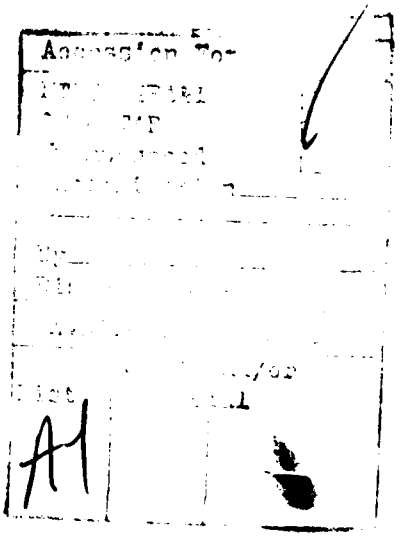

BEHAVIOR OF IONIZED PLASMA IN THE HIGH LATITUDE TOPSIDE IONOSPHERE

I. INTRODUCTION

The behavior of plasma on the auroral magnetic field lines has been the subject of a number of studies in recent years. Theoretical models of the polar wind have been developed by Banks and Holzer [1968, 1969], Holzer et al., [1971], and Lemaire and Scherer [1973]. Using the 13-moment system of transport equations of Schunk [1977], Schunk and Watkins [1981, 1982] have studied the steady state flow of a fully ionized H^+ - O^+ - electron plasma along geomagnetic field lines. In their first study of the polar wind [1981] they used the 13-moment equations for the electron gas and a simplified set of transport equations for the hydrogen and oxygen ions. Their results show that electron temperature anisotropy develops at altitudes above 2500 km. Below 2500 km the electron gas is essentially collision dominated. In their next study of the polar wind [1982] they have used the 13-moment system of equations for the hydrogen ions also. The results show that for supersonic flow at high altitudes the hydrogen ion temperature parallel to the field line ($T_{p_\parallel}$) is greater than the temperature perpendicular to the field line ($T_{p_\perp}$). The reverse is true for subsonic flow.

Using the same 13-moment system of equations, Mitchell & Palmadesso [1983] developed a dynamic numerical model of the plasma along an auroral field line. The plasma consists of the electrons, hydrogen and oxygen ions. The electrons and the hydrogen ions are the dynamic species in the model. They have performed simulations for the case of a current-free

Manuscript approved May 23, 1985.

polar wind and the case in which an upward field - aligned current was applied along the field line. The results of the polar wind simulations have been compared to those of Schunk and Watkins [1981, 1982]. It is seen that for low electron temperature and supersonic hydrogen ion outflow, both exhibit an anisotropic hydrogen ion cooling and both have a region in which the parallel temperature increases with altitude before adiabatic cooling dominates. The electron temperature profiles, however, cannot be directly compared. The lower boundary of Mitchell and Palmadesso [1983] was held at a constant temperature and the simulation was run until a steady-state was achieved. The outflow condition treats the upper boundary as an electron heat sink and therefore the electron temperature decreases with altitude. Schunk and Watkins [1981] specified the electron temperature and a positive electron temperature gradient at the lower end, as the initial condition to study the electron temperature anisotropy. The upper boundary need not be specified in this case.

We have developed a numerical model to study the steady state behavior of the plasma encompassing geomagnetic field lines. The theoretical formulation used is based on the 16-moment system of transport equations of Schunk et al. [1982]. The 13-moment system of transport equations allow for different species temperature parallel and perpendicular to the field line, but allow only a single heat flow per species. The 16-moment equations allow transverse and parallel thermal energy to be transported separately, which simulates the behavior of a large temperature anisotropy for a collisionless plasma better than the 13-moment equations. This is expected to be an important advantage in studies of auroral field aligned transport which include the effects of return currents and anomalous transport processes, such as anomalous resistivity and associated

anisotropic heating. Such studies are now in progress, and will be the subject of a future report. We have used this model to perform polar wind simulations. This to our knowledge is the first successful steady state solution to the 16 moment set of transport equations for the polar wind problem.

II. THE MODEL

A numerical model has been developed to simulate the steady state behavior of a fully ionized plasma (H^+, O^+ and the electrons) along the geomagnetic field lines in the high latitude topside ionosphere. The electrons and the hydrogen ions are the dynamic species in the model and the oxygen ions form a static background population at a constant temperature. The H^+ and electron temperature anisotropies and heat flows are not sensitive to the oxygen temperature and heat flows, as noted by Schunk and Watkins [1981, 1982]. Thus maintaining the O^+ ions at a constant temperature did not introduce appreciable errors as far as the H^+ ions and the electrons are conerned [Schunk 1982].

The distribution function is considered to be gyrotropic about the field line direction, which reduces the 16-moments approximation to six moments: number density, velocity of the species parallel to the field line, temperature pa.allel and perpendicular to the field line, and parallel and perpendicular heat flow along the field line. The resulting transport equations used for hydrogen and electrons are given as follows

$$\frac{\partial n}{\partial t} + \frac{\partial nv}{\partial r} + \dot{A}nv = \frac{\delta n}{\delta t} \qquad (1)$$

$$\frac{\partial v}{\partial t} + v\frac{\partial v}{\partial r} + \frac{k}{mn}\frac{\partial nT_{\parallel}}{\partial r} + \frac{GM}{r^2} - \frac{eE}{m} + \frac{\dot{A}k}{m}(T_{\parallel} - T_{\perp}) = \frac{\delta v}{\delta t} \qquad (2)$$

$$k\frac{\partial T_{\parallel}}{\partial t} + kv\frac{\partial T_{\parallel}}{\partial r} + \frac{2}{n}\frac{\partial nh_{\parallel}}{\partial r} + 2\dot{A}(h_{\parallel} - h_{\perp}) + 2kT_{\parallel}\frac{\partial v}{\partial r} = k\frac{\delta T_{\parallel}}{\delta t} \qquad (3)$$

$$k\frac{\partial T_{\perp}}{\partial t} + kv\frac{\partial T_{\perp}}{\partial r} + \frac{1}{n}\frac{\partial nh_{\perp}}{\partial r} + \dot{A}(2h_{\perp} + kT_{\perp}v) = k\frac{\delta T_{\perp}}{\delta t} \qquad (4)$$

$$\frac{\partial h_{\parallel}}{\partial t} + v\frac{\partial h_{\parallel}}{\partial r} + 3h_{\parallel}\frac{\partial v}{\partial r} + \frac{3}{2}\frac{k^2T_{\parallel}}{m}\frac{\partial T_{\parallel}}{\partial r} = \frac{\delta h_{\parallel}}{\delta t} \qquad (5)$$

$$\frac{\partial h_{\perp}}{\partial t} + v\frac{\partial h_{\perp}}{\partial r} + h_{\perp}\frac{\partial v}{\partial r} + \frac{k^2T_{\perp}}{m}\frac{\partial T_{\perp}}{\partial r} + \dot{A}(vh_{\perp} + \frac{T_{\perp}k^2}{m}(T_{\parallel} - T_{\perp})) = \frac{\delta h_{\parallel}}{\delta t} \qquad (6)$$

Charge neutrality

$$n_e = n_p + n_o \qquad (7)$$

where, n = number density

v = species velocity

A = cross-sectional area of a flux tube (proportional to 1/B)

B = magnetic field of the earth

E = Electric field parallel to the field line

G = gravitational constant

M = mass of the earth

m = mass of the particular species

$T_{\parallel}$ = temperature of the species parallel to the field line

$T_{\perp}$ = temperature of the species perpendicular to the field line

$h_{\parallel}$ = heat flow parallel to the field line

$h_{\perp}$ = heat flow perpendicular to the field line

k = Blotzmann constant

$\dot{A} = \frac{1}{A}\frac{\partial A}{\partial r} = \frac{3}{r}$

e = electrons

p = hydrogen ions

o = oxygen ions

For a given moment F of the distribution function, $\delta F/\delta t$ represents the change in F due to the effects of collisions and may also include anomalous transport effects associated with plasma turbulence. The collision terms used in this model are those of Mitchell and Palmadesso [1983]. They have used Burger's [1979] collision terms for the case of Coulomb collisions with corrections for finite species velocity differences. The collision terms are given in Appendix A.

We have assumed that the total flux tube current I remains constant

$$I = eA(n_p v_p - n_e v_e) \tag{8}$$

which implies

$$v_e = \frac{1}{n_e}\left(n_p v_p - \frac{I}{eA}\right) \tag{9}$$

In the following, the current I is assumed to be zero

Using equations (2), (7) and (8) the electric field E parallel to the field line is calculated [Mitchell and Palmadesso, 1983].

$$E = \frac{m_s}{en_eA}\frac{\partial}{\partial r}(n_pv_p^2A - n_ev_e^2A) - \frac{k}{e}\left[\frac{\partial T_{e\parallel}}{\partial r} + \frac{T_{e\parallel}}{n_e}\frac{\partial n_e}{\partial r}\right.$$

$$\left. + \frac{(T_{e\parallel} - T_{e\perp})}{A}\frac{\partial A}{\partial r}\right] - \frac{n_om_eGM}{n_eer^2} + \frac{m_e}{e}\left[\frac{\delta v_e}{\delta t} - \frac{n_p}{n_e}\frac{\delta v_p}{\delta t}\right] \qquad (10)$$

We will consider the steady state solutions of the equations (1)-(6). This set of ordinary differential equations are solved by first eliminating all derivatives in a given equation except one and then integrating the resulting quatities numerically along the field line. The new set of equations are:

$$\frac{\partial n_p}{\partial r} = -\frac{n_p}{v_p}\frac{\partial v_p}{\partial r} - \frac{3}{r}n_p \qquad (i)$$

$$\frac{\partial v_p}{\partial r} = \frac{1}{\left[v_p - \frac{k\,T_{p_\parallel}}{v_pm_p} - \frac{T_{e_\parallel}\,k\,n_p}{m_pv_p(n_o + n_p)}\right]}$$

$$\left[\frac{3k\,T_{p_\parallel}}{r\,m_p} + \frac{3\,k\,T_{e_\parallel}\,n_p}{r\,m_p\,(n_p + n_o)} - \frac{k}{m_p}\frac{\partial T_{p_\parallel}}{\partial r}\right.$$

$$\left. - \frac{k}{m_p}\frac{\partial T_{e_\parallel}}{\partial r} - \frac{k\,T_{e_\parallel}}{m_p(n_o + n_p)}\frac{\partial n_o}{\partial r} - \frac{3k}{rm_p}(T_{e_\parallel} - T_{e_\perp})\right.$$

$$- \frac{n_o m_e \, GM}{m_p r^2 \, (n_o + n_p)} - \frac{GM}{r^2} + \frac{m_e}{m_p} \frac{\delta v_e}{\delta t}$$

$$+ \left[1 - \frac{m_e \, n_p}{m_p (n_o + n_p)} \right] \frac{\delta v_p}{\delta t} - \frac{3k \, (T_{p_\parallel} - T_{p_\perp})}{r m_p} \Bigg] \qquad \text{(ii)}$$

$$\frac{\partial T_\parallel}{\partial r} = \frac{1}{\left[kv - \frac{3k^2}{v} \frac{T_\parallel}{m} \right]} \left[- \frac{2}{n} h_\parallel \frac{\partial n}{\partial r} + \frac{6}{r} (h_\perp - h_\parallel) \right.$$

$$\left. - \left[2T_\parallel k - \frac{6h_\parallel}{v} \right] \frac{\partial v}{\partial r} + k \frac{\delta T_\parallel}{\delta t} - \frac{2}{v} \frac{\delta h_\parallel}{\delta t} \right] \qquad \text{(iii)}$$

$$\frac{\partial T_\perp}{\partial r} = \frac{1}{\left[kv - \frac{k^2 T_\parallel}{m \, v} \right]} \left[\frac{h_\perp}{v} \frac{\partial v}{\partial r} - \frac{h_\perp}{n} \frac{\partial n}{\partial r} - \frac{3}{r} h_\perp - \frac{3k \, T_\perp \, v}{r} \right. \qquad \text{(iv)}$$

$$\left. + \frac{3k^2 T_\perp}{mrv} (T_\parallel - T_\perp) + k \frac{\delta T_\perp}{\delta t} - \frac{1}{v} \frac{\delta h_\perp}{\delta t} \right]$$

$$\frac{\partial h_\parallel}{\partial r} = - \frac{3h_\parallel}{v} \frac{\partial v}{\partial r} - \frac{3}{2} \frac{k^2}{v} \frac{T_\parallel}{m} \frac{\partial T_\parallel}{\partial r} + \frac{1}{v} \frac{\delta h_\parallel}{\delta t} \qquad \text{(v)}$$

$$\frac{\partial h_\perp}{\partial r} = -\frac{h_\perp}{v}\frac{\partial v}{\partial r} - \frac{k^2 T_\parallel}{v\, m}\frac{\partial T_\perp}{\partial r}$$

$$-\frac{3}{r}h_\perp - \frac{3k^2\, T_\perp}{v\, r\, m}(T_\parallel - T_\perp) + \frac{1}{v}\frac{\partial h_\perp}{\partial t} \qquad \text{(vi)}$$

The simulation is carried out on an unequally spaced grid, with smaller cell sizes at the lower end of the flux tube. This enables us to determine the plasma dynamics properly in the presence of large density gradients due to the small scale height of oxygen.

The equations we have to solve represents a system of stiff differential equations. A typical solution of a stiff system has a short initial interval in which it changes rapidly (called an initial transient) after which it settles down to a comparatively slowly varying state. Methods of solving stiff ordinary differential equations has been discussed by Gear et al., [1979]. We will use the general procedure used by Watkins [1981].

III. SIMULATIONS AND RESULTS

Schunk and Watkins [1982] have performed polar wind simulations for both supersonic and subsonic hydrogen ion outflow. Until recently it was not clear if the polar wind is supersonic or subsonic. Nagai et al. [1984] first reported the supersonic nature of the polar wind along polar cap field lines. The data for this study were obtained from DE 1 satellite.

This paper clearly shows that the hydrogen ion flow in the polar ionosphere is supersonic in nature. Subsonic polar wind has not yet been observed. We shall thus consider hydrogen ion outflow as supersonic

As noted above, solutions have been obtained for the current free case. The lower boundary is fixed at 1500 km. At this boundary we set H^+ ion velocity at 16 km s^{-1}, H^+ ion density at 80 cm^{-3}, and oxygen ion density at 5000 cm^{-3}. The hydrogen ion temperature at the lower boundary is 3500°K. The oxygen ion temperature was kept constant at 1200°K. The results of this current free polar wind simulation are shown in figures 1a-1g. Figure 1a shows oxygen ion density, 1b shows H^+ ion density, 1c shows electron density, 1d shows hydrogen ion velocity. Oxygen ions are the dominant species only up to an altitude of 3500 km. Supersonic H^+ ions flow in divergent magnetic field lines. The hydrogen momentum balance equation shows that the ambipolar electric field value produces the sharp increase in H^+ ion velocity at the lower end of the tube. Electron velocity also increases as is evident from equation (9) and is shown in Figure 1e. The total flux along the flux tube is conserved, i.e., nVA = constant. Therefore, as the velocity and the area increases the density should decrease. The hydrogen ion density decreases as it flows through the diverging flux tube. The electron density also decreases, as is evident from the charge neutrality equation (7).

A study of equation (ii) reveals that at the upper end of the flux tube the velocity variation is driven mainly by the terms containing the hydrogen ion temperature difference ($T_{p_\parallel} - T_{p_\perp}$), electron temperature difference ($T_{e_\parallel} - T_{e_\perp}$), hydrogen ion temperature ($T_{p_\parallel}$) and electron temperature ($T_{e_\parallel}$) parallel to the field line, i.e., mirror forces and parallel pressure gradients.

Figure 1f shows the hydrogen ion temperature parallel and perpendicular to the geomagnetic field. The hydrogen ion temperature exhibits two basic characteristics:

(1) Adiabatic cooling - Supersonic ion gas cools down as it expands in a diverging magnetic field

(2) Temperature anisotropy

These effects were also displayed by the previous studies of the polar wind using the 13-moment system of equations by Schunk and Watkins [1982] and Mitchell and Palmadesso [1982]. Like Schunk and Watkins [1982], we obtained solutions for only positive H^+ heat flow at the lower boundary. This implies that an upward flow of heat from the lower ionosphere is required for a supersonic hydrogen ion outflow [Schunk, 1982]. This upward flow of heat is associated with a negative H^+ temperature gradient.

At the lower end of the flux tube, due to rapid expansion of the supersonic ion gas, both $T_\perp$ and $T_\parallel$ decrease. This was also noted by Schunk and Watkins [1982]. The hydrogen ion temperature perpendicular to the field line decreases continuously. Appreciable temperature anisotropy develops around 2500 km . The temperature anisotropy is more prominent in the H^+ ions than in the electrons. This is because of the fact that the hydrogen ions have supersonic velocities and in the collisionless region heat transport is not efficient for H^+ ions, compared to that for electrons. Also, as the particles move up in a decreasing magnetic field, $v_\perp$ decreases in order to keep adiabatic invariant μ constant. As the total energy of the particle is conserved, $\frac{1}{2} m v_\perp^2$ decreases with the increase of $\frac{1}{2} m v_\parallel^2$. That is, perpendicular energy gets converted to parallel energy. A study of equation (iii) and (iv) show that the temperature variation is produced mainly as a balance between the

convection process and the mirror force effects. The collisions play an important role below 2500 km. In equations (v) and (vi) the temperature gradient terms are very important.

We compared our solution of the equations based on the 16-moment system with that of Schunk and Watkins [1982] solution of the 13-moment equations. The general behavior of the H^+ ion temperature parallel and perpendicular to the field line remains the same. H^+ ion temperature perpendicular to the field line decreases continuously with altitude. Parallel temperature first decreases and then increases and finally tends to remain constant with altitude. We observe an anisotropy with $T_\perp > T_\parallel$ below 2500 km. Schunk and Watkins [1982] observed similar anisotropy for the low electron temperature case when they lowered the H^+ ion temperature and heat flow and when the oxygen ion density was increased at the lower end. They have pointed out that the results are sensitive to the boundary conditions used, in the sense that the qualitative picture remains the same only the quantitative picture differs.

We have also compared our results with those of Mitchell and Palmadesso [1983] and Holzer et al. [1971]. Mitchell and Palmadesso [1983] started their simulation at 800 km at the lower boundary. At this level the H^+ ion temperature increases with altitude due to Joule heating caused by H^+ ion collisions with oxygen ions. This effect rapidly decreases with altitude. The general qualitative picture here is in good agreement with our results.

Holzer et al. [1971] have compared the solutions of hydrodynamic and kinetic solutions for supersonic polar wind outflow in a collisionless regime. Both hydrodynamic and kinetic solutions show that $T_\perp$ decreases continuously. $T_\parallel$ for both cases decreases rapidly with altitude and then

tends to become constant. For the hydrodynamic case at all altitudes the hydrogen ion temperature parallel to the field line was greater than that perpendicular to the field line. The kinetic solutions showed a region at the lower end where $T_\perp$ was greater than $T_\parallel$. The cross-over region was noticed at the lower end. In these cases also we notice that our solutions are in good agreement with Holzer et al, [1971].

Finally, we compared our results with Nagai et al. [1984]. Nagai et al. [1981] have used the data from Dynamics Explorer (DE) to demonstrate the supersonic nature of the polar wind. The observations were obtained from 65° to 81° invariant latitute and an altitude near $2R_E$. The results show that for an estimated range of spacecraft potential of + 3 to +5V, the temperature range of 0.1 to 0.2 eV was obtained corresponding to flow velocities of 25 to 16 km s^{-1}. Calculated Mach numbers ranged from 5.1 to 2.6. The Mach number calculated from our results corresponding to a flow velocity of 16 km per second is 2.2.

We have varied slightly the H^+ ion velocity, density and temperature at the lower end to study the sensitivity of the solutions, to these parameters. At the lower end the hydrogen ion density is increased to 100 cm^{-3}, velocity is decreased to 10 km per second and the temperature is raised to 3800°K. The results of these changes are presented in figures 2a-2f. The qualitative picture and the relative importance of the contributing terms remain the same as before. The quantitative change is obvious as the initial conditions are changed. The mach number calculated in this case of a flow velocity of 16 km s^{-1} is 2.68. This is in good agreement with the value 2.6 calculated by Nagal et al. [1984].

Electron temperature parallel and perpendicular to the geomagnetic field lines are shown in Figure 1g. The most important effect exhibited by

electron temperature is :

(1) temperature anisotropy

(2) Below 2500 km the electron gas is collision dominated, as noted by Schunk et al. [1981]

"Collision dominated" implies that the collision relaxation rate is greater than the rate associated with the driving term that produces the anisotropy. Appreciable temperature anisotropy develops above 2500 km. Both temperature parallel and perpendicular to the field line increases. Heat flow is considered downward here (that is, heat flows from the magnetosphere to the ionosphere) as considered by Schunk et al. [1981]. Also as noticed by Schunk et al. [1981], the electron temperature ratio at the upper end is $T_\perp/T_\parallel - 2$. The contributions from the collision term are very important below 2500 km in equations (iii) and (iv). Since the collision terms are important in this region, the electron temperature anisotropy observed in this region is very small. The anisotropy increases with altitude. Electron temperature variation is produced mainly as a balance between the convection process and the mirror force process. The heat flow is downward for the electrons and the perpendicular energy increases as the parallel energy decreases. The temperature gradient terms are important at all altitudes in equations (v) and (vi) the electron species velocity is less than the electron thermal velocity.

Our results here are in good agreement with Schunk and Watkins [1981] low electron temperature case. Schunk and Watkins [1981] varied the boundary electron temperature gradients to see the extent to which their solutions are valid. Their results show that with the increase in boundary electron temperature gradient, the electron temperature increased but the direction of anisotropy remained the same. It is also clearly explained by

Schunk and Watkins [1981] that this observed anisotropy is opposite to that predicted by the Chew-Goldgerger-Low (double adiabatic) energy equations. The tendency of the adiabatic terms to produce an anisotropy with $T_{\parallel} > T_{\perp}$ is also present in our equations, but the heat flow effects dominate and act to produce the reverse anisotropy.

The electron temperature profiles cannot be directly compared to Mitchell and Palmadesso [1983]. They treated the upper boundary as an electron heat sink, which decreases the electron temperature with altitude.

IV. DISCUSSIONS

We have studied the steady state behavior of the plasma encompassing the geomagnetic field lines using equations based on the 16-moment system of transport equations. The asymptotic behavior of the solutions of the transport equations at high altitudes is quite sensitive to the boundary conditions applied at the lower end of the flux tube. This, coupled with with absence of any standard set of assumptions for specifying those dynamic variables for which upper boundary conditions must be supplied, leads to considerable variation of the results at high altitudes in the studies referenced above. Effectively, one finds similar ionospheres and widely different magnetospheres in this group of calculations. While this makes quantitative comparison of results somewhat difficult, it is clear that qualitative agreement among the various calculations is good.

Studies of auroral field line equilibria including the effects of return currents and anomalous transport processes, and using the 16 moment approach described here, are in progress.

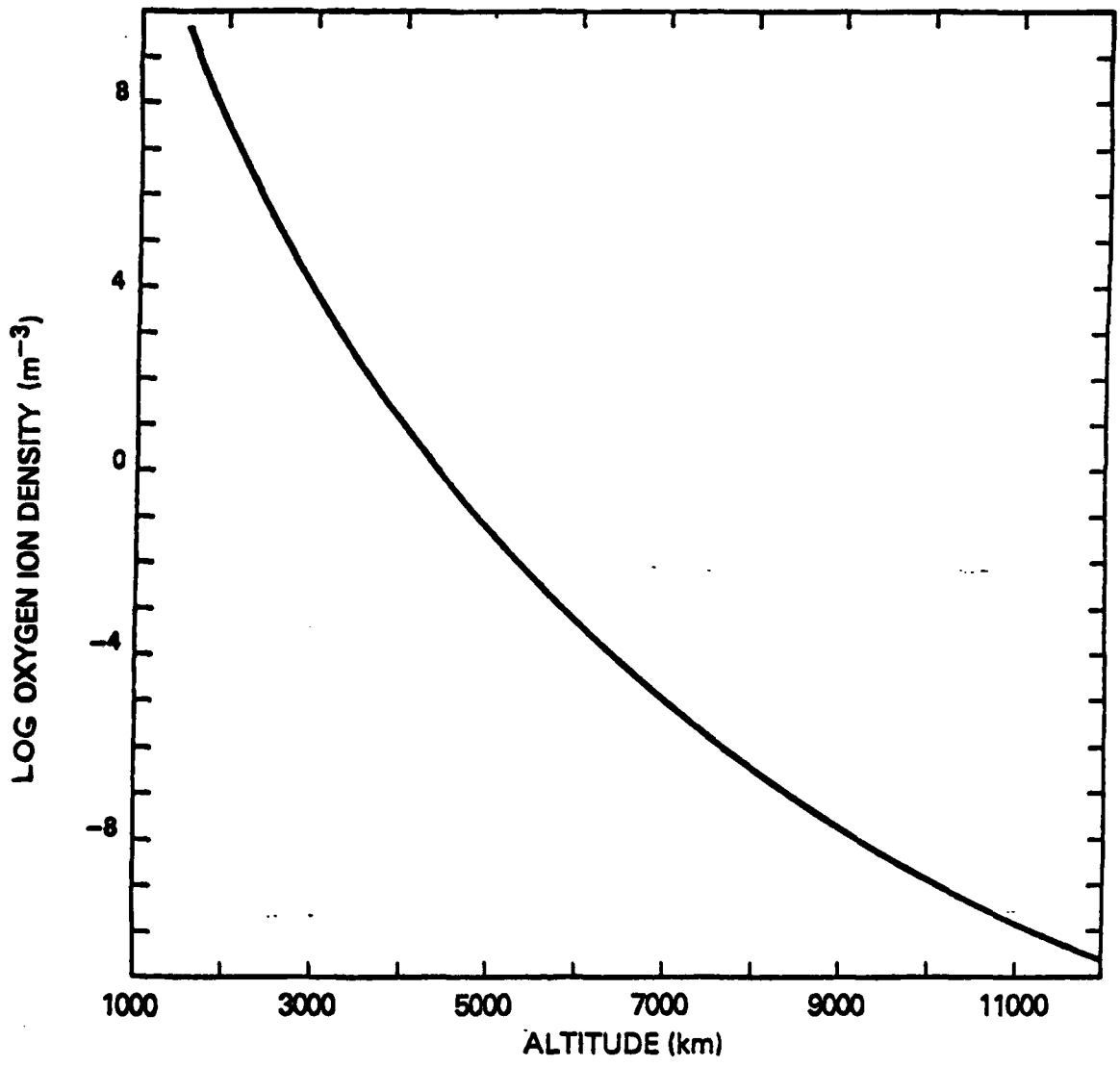

Fig. 1(a) — Oxygen ion density profile for steady state polar wind

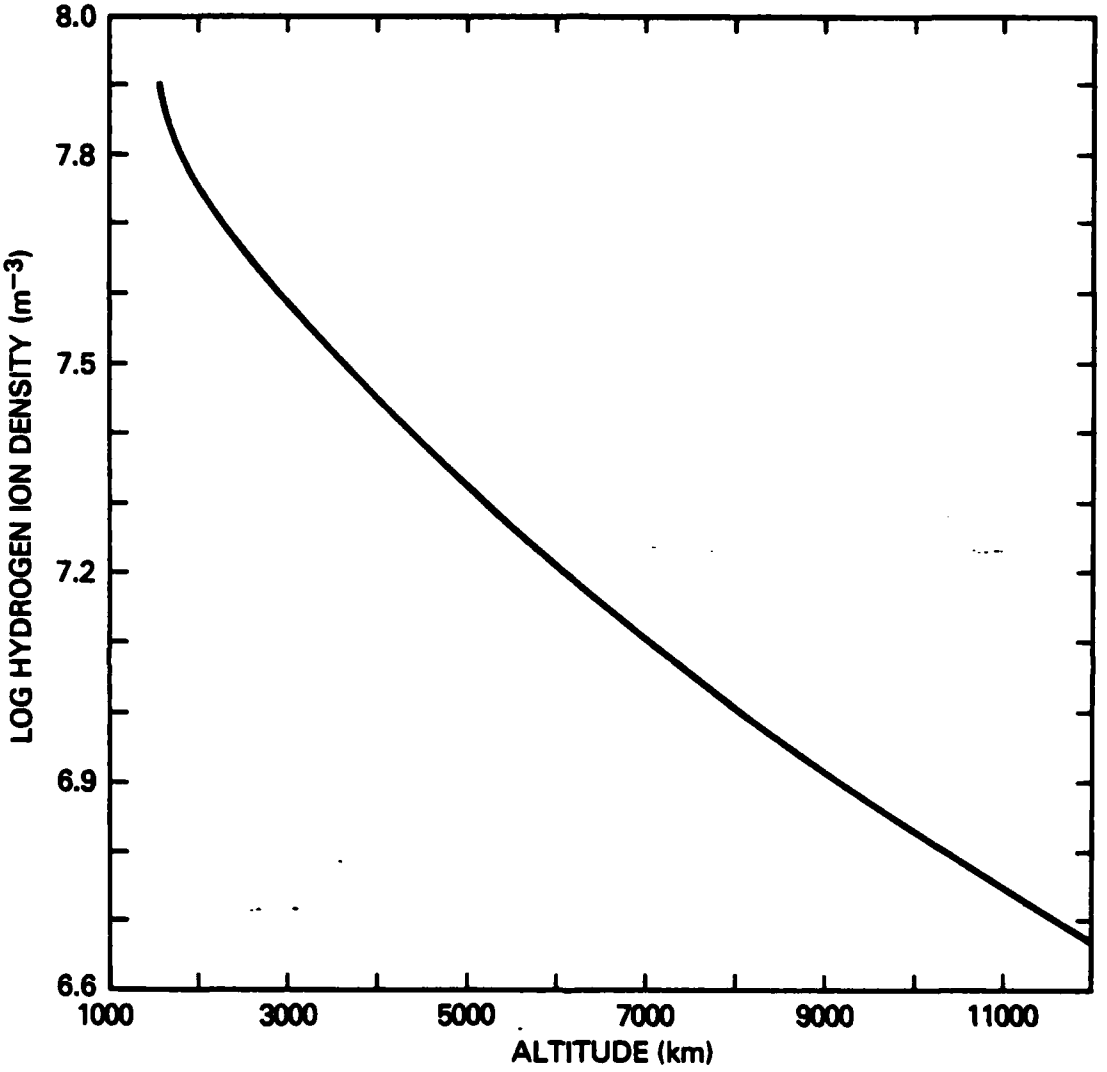

Fig. 1(b) — H^+ ion density profile versus altitude

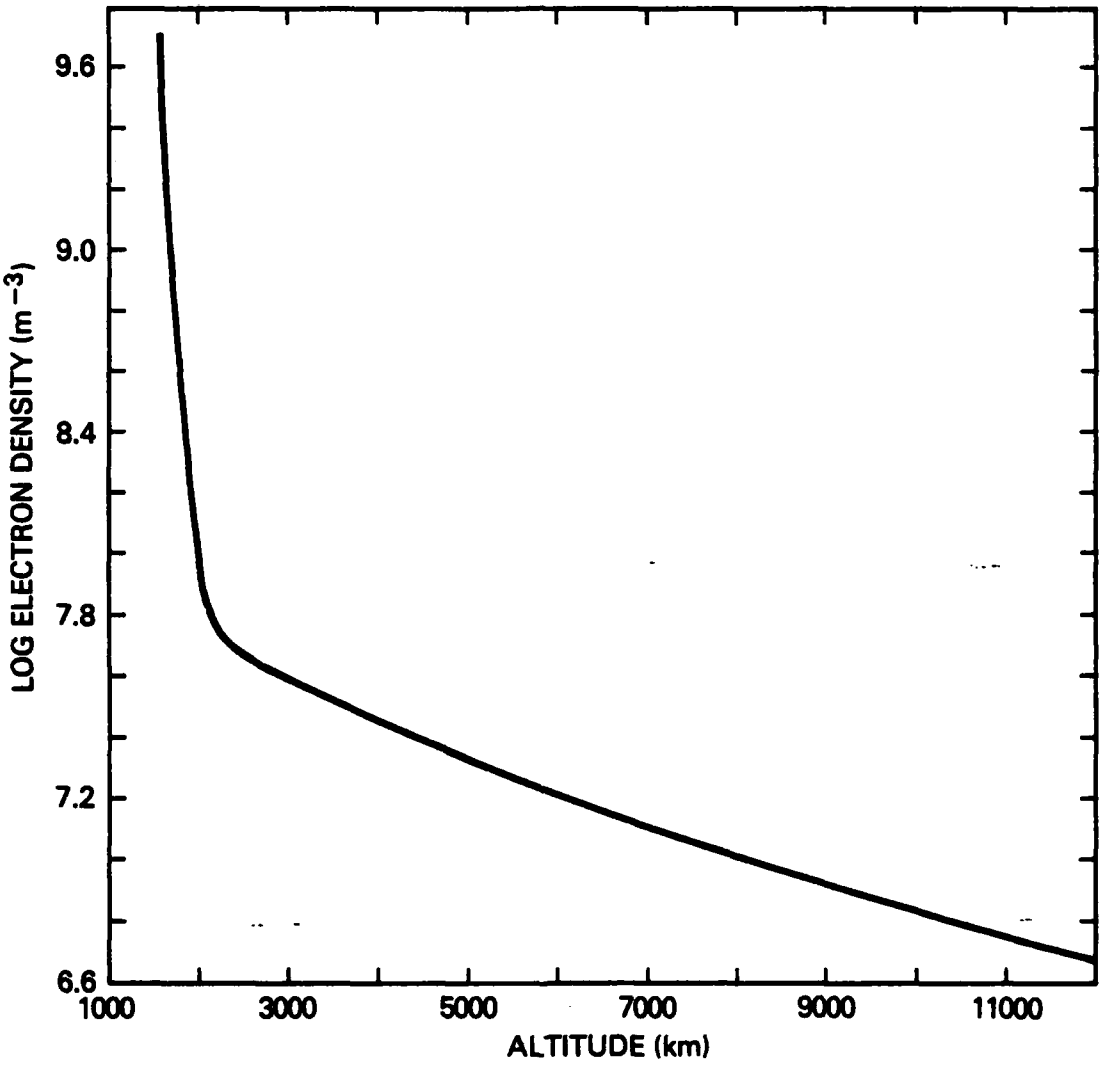

Fig. 1(c) — e^- density profile

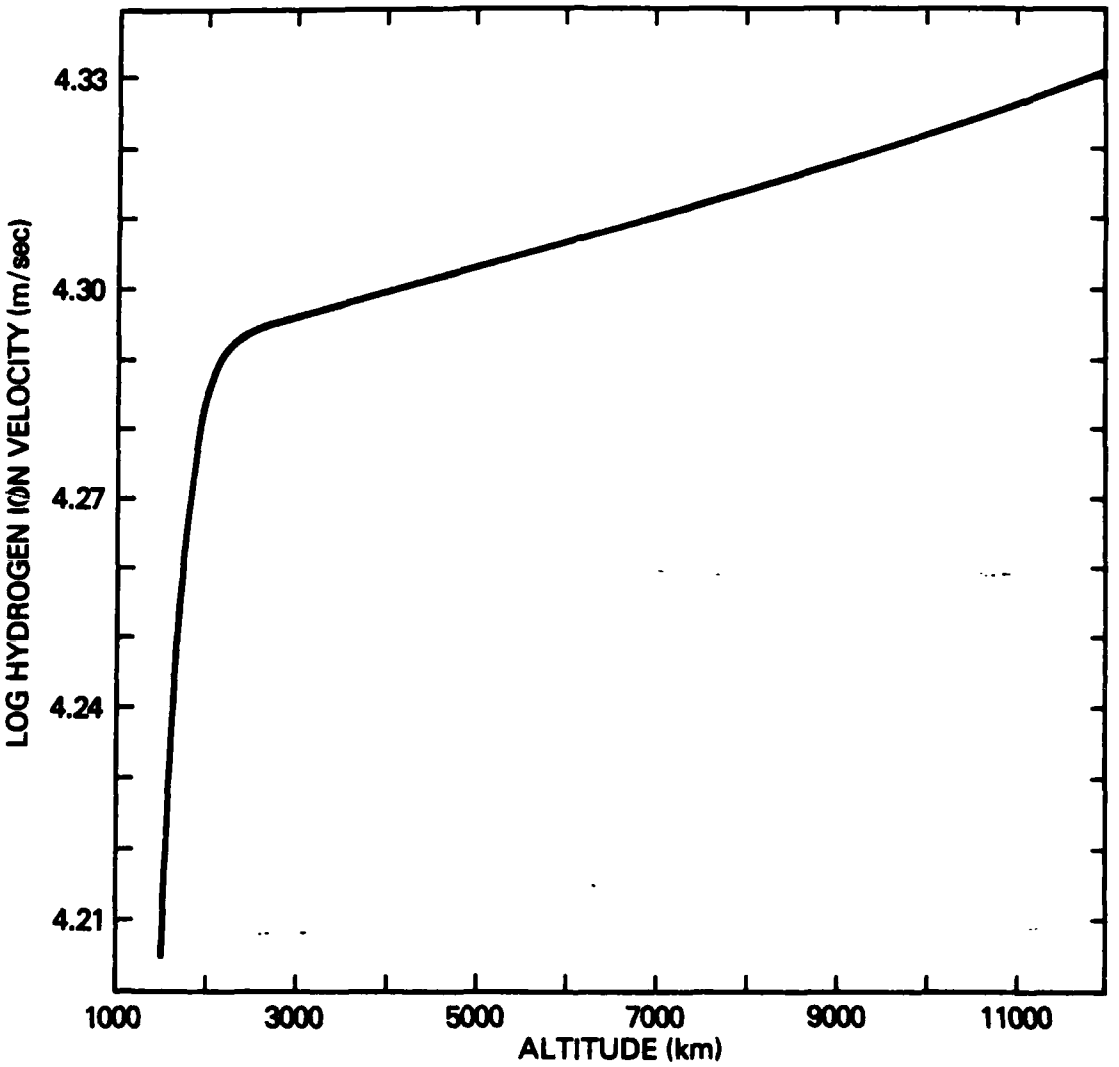

Fig. 1(d) — H^+ velocity profile for steady state polar wind

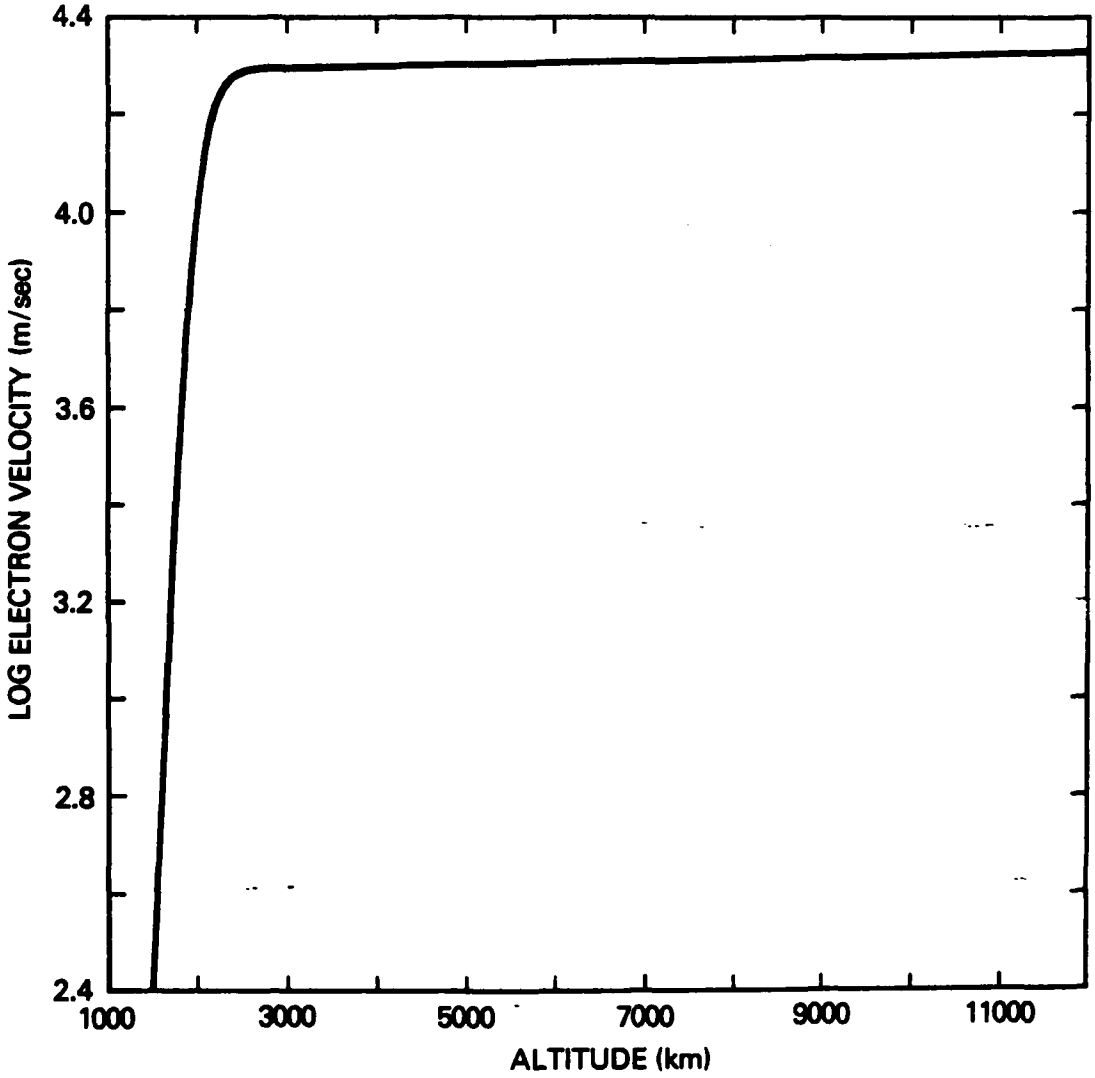

Fig. 1(e) — e^- velocity profile versus altitude

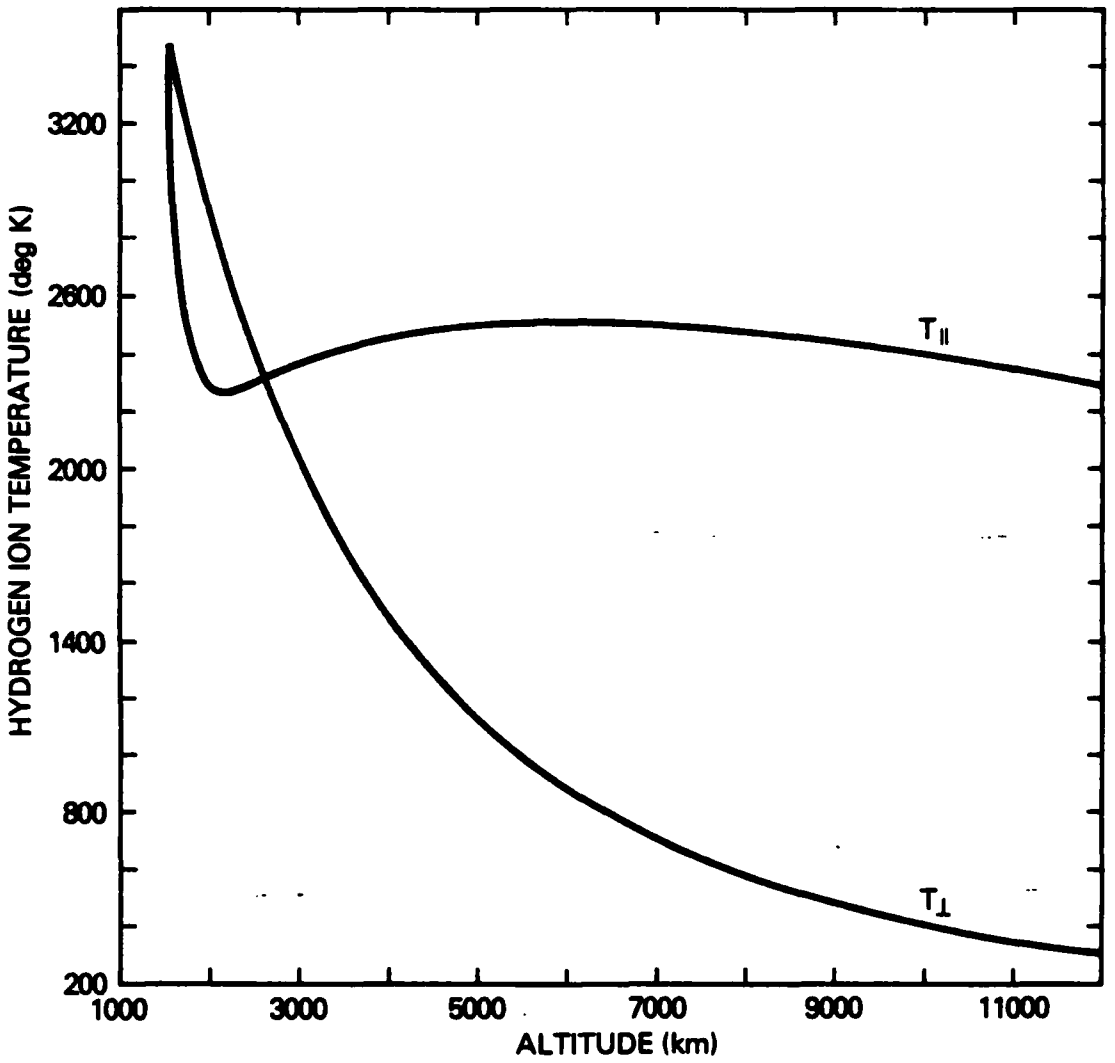

Fig. 1(f) — H^+ ion temperature parallel and perpendicular to the geomagnetic field versus altitude

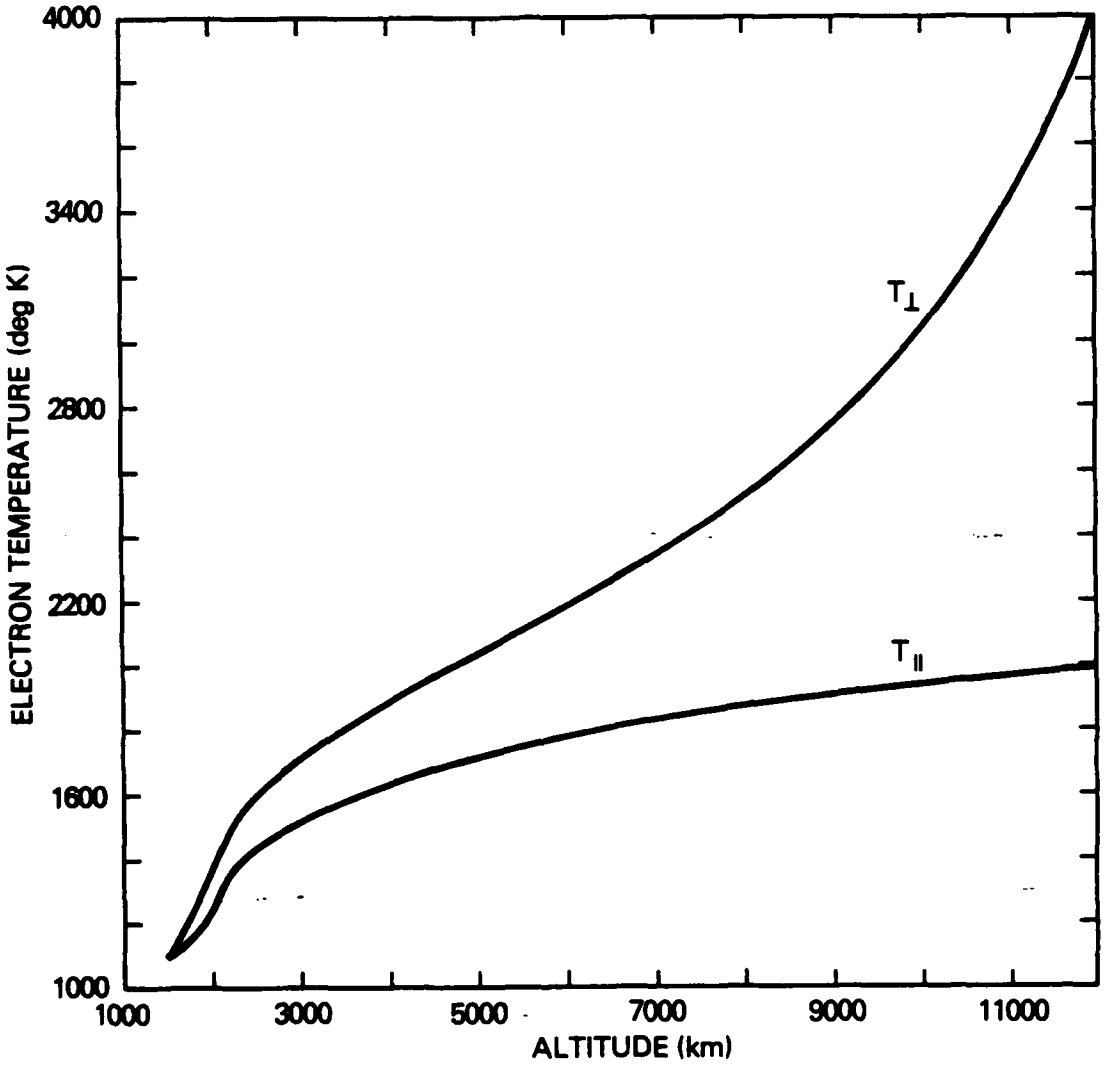

Fig. 1(g) — e^- temperature parallel and perpendicular to the geomagnetic field versus altitude

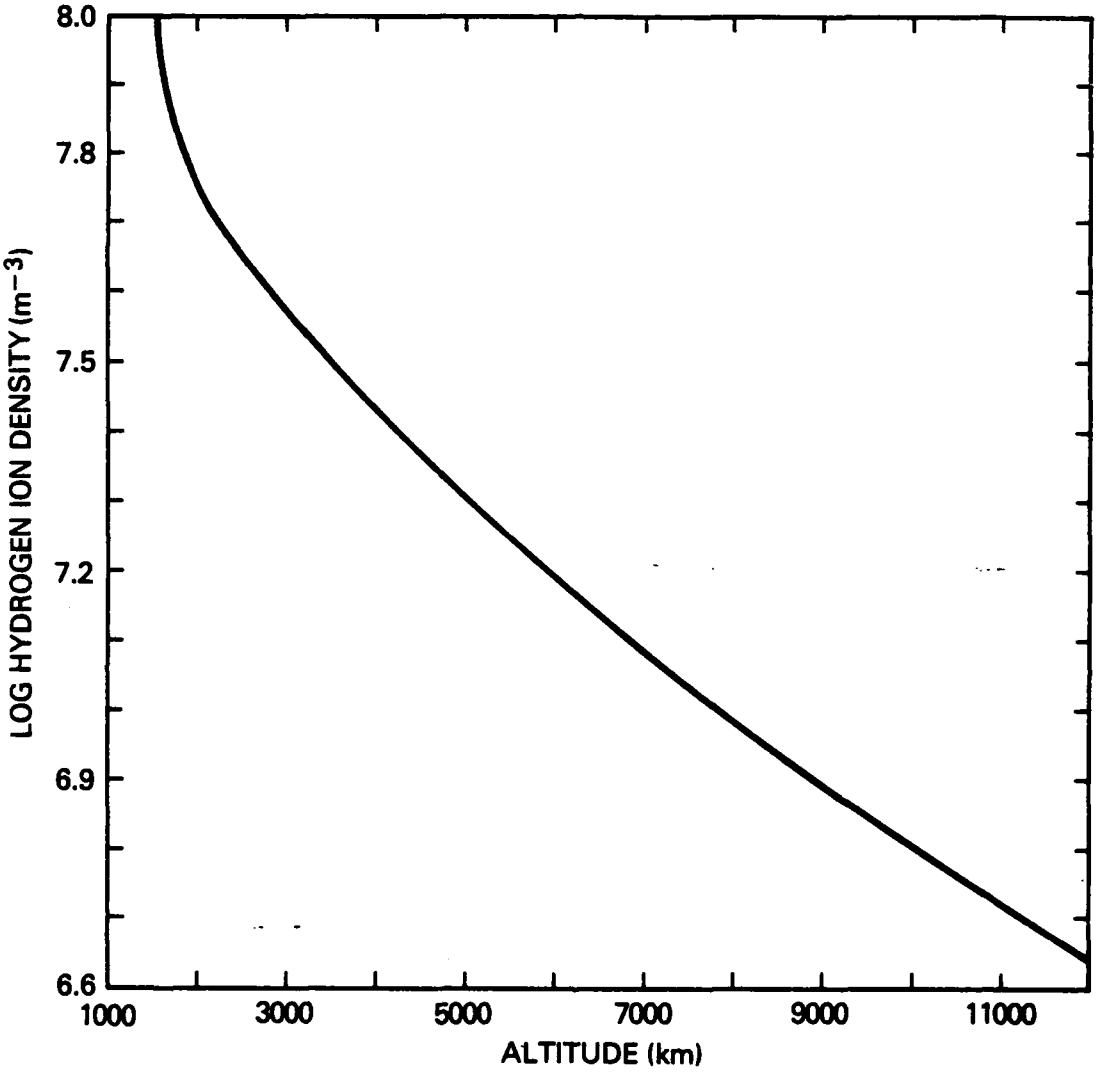

Fig. 2(a) — H^+ ion density profile for steady state polar wind versus altitude

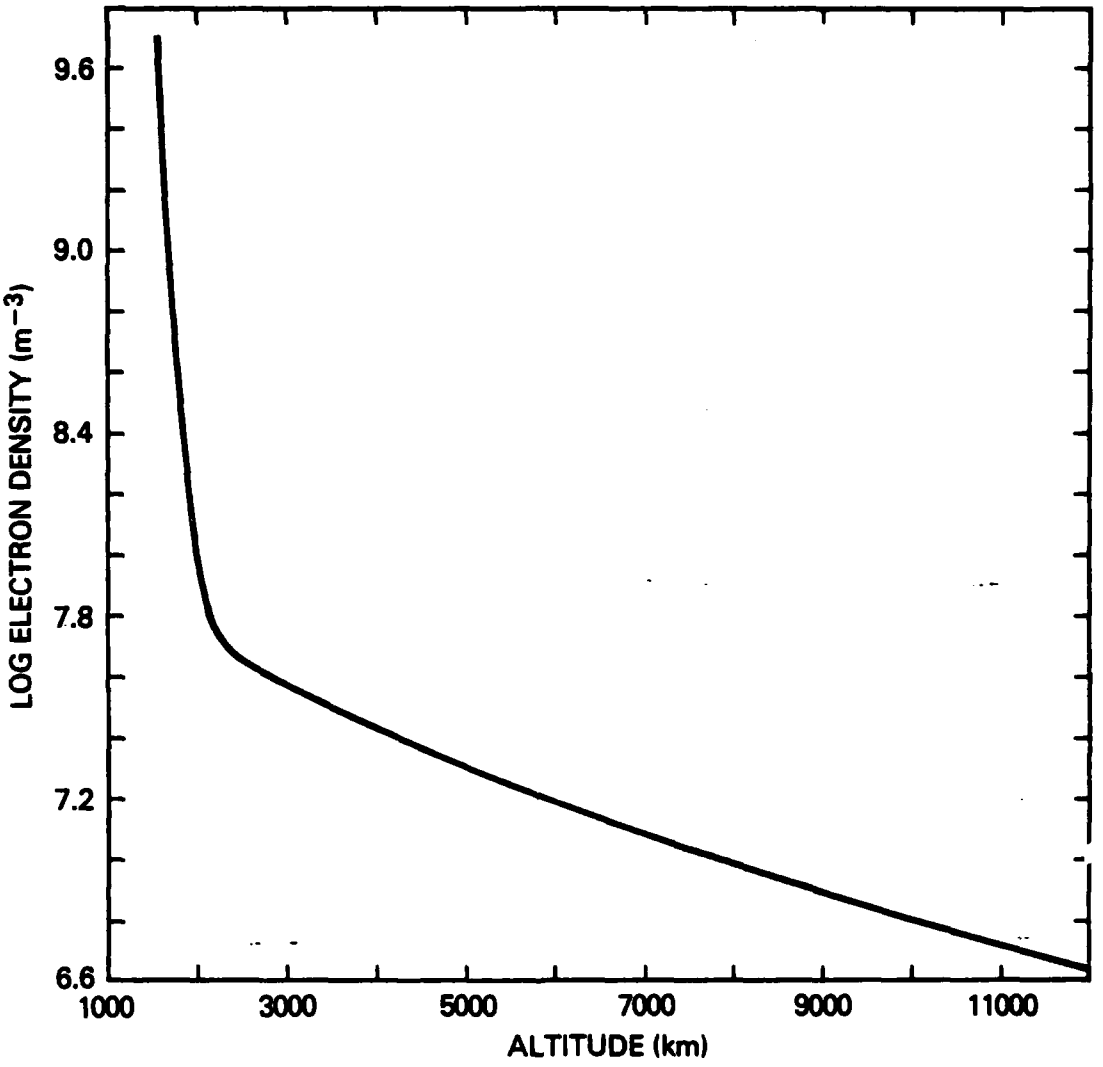

Fig. 2(b) — e^- density profile

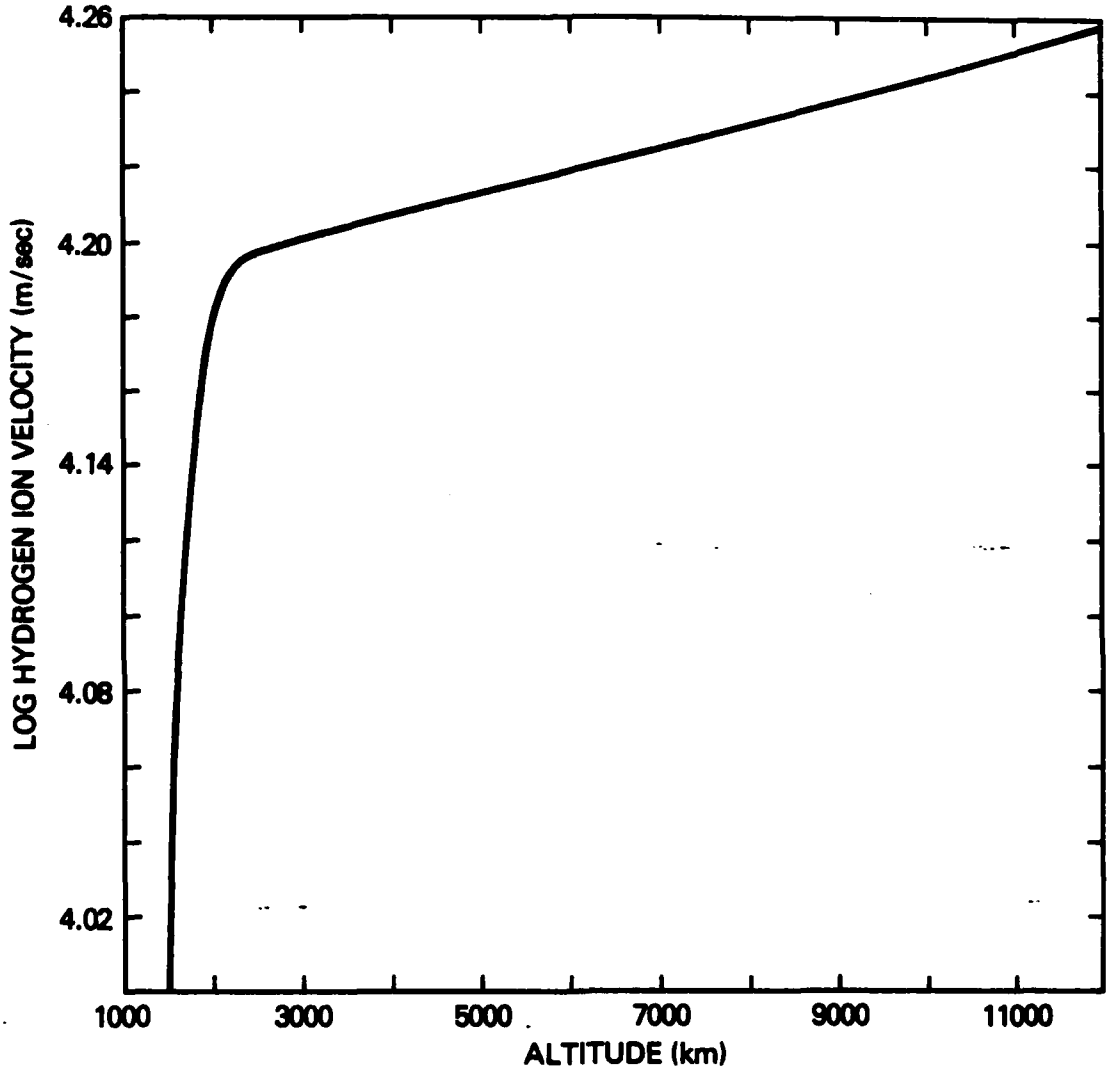

Fig. 2(c) — H^+ ion velocity profile

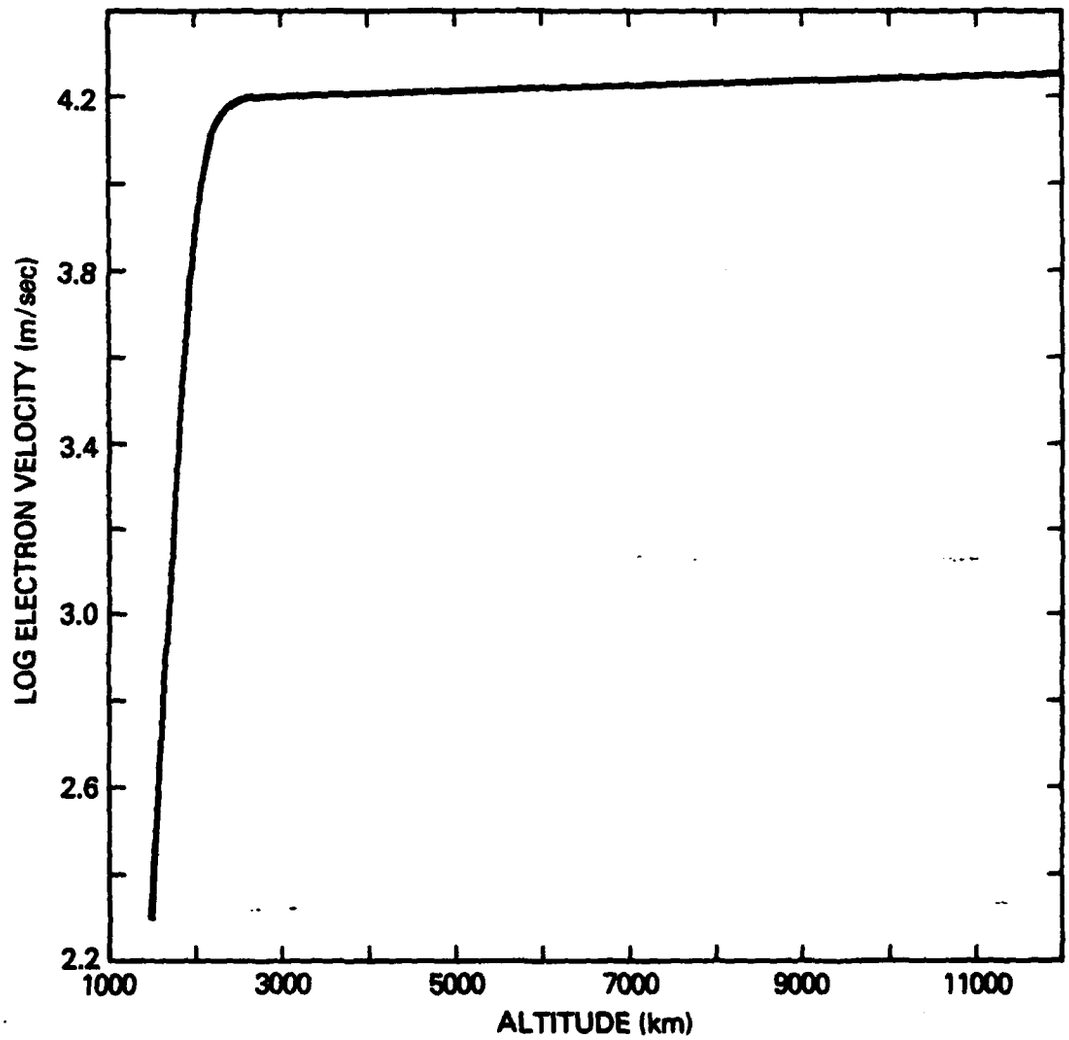

Fig. 2(d) — e^- density profile

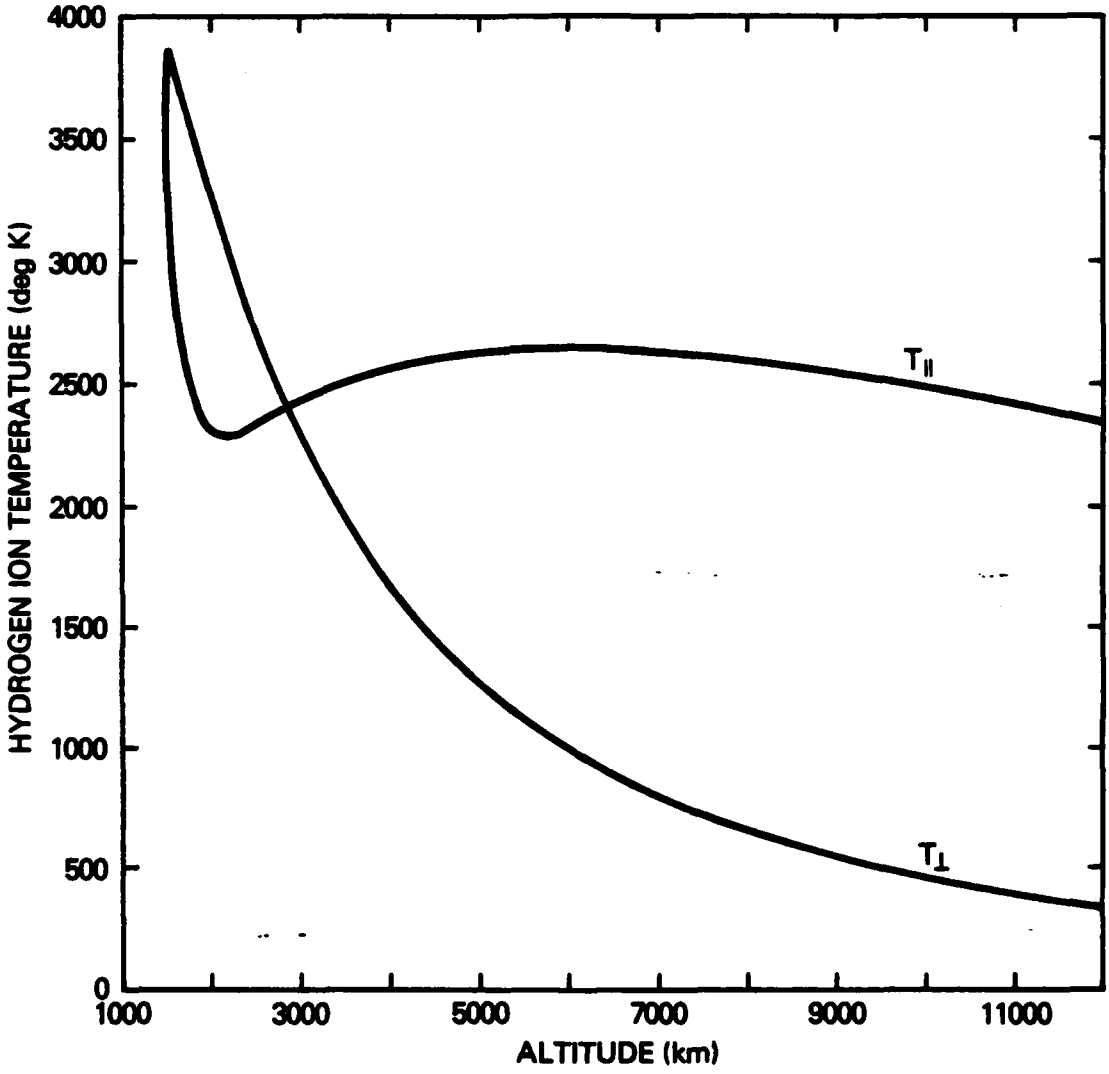

Fig. 2(e) — H^+ ion temperature parallel and perpendicular to the geomagnetic field

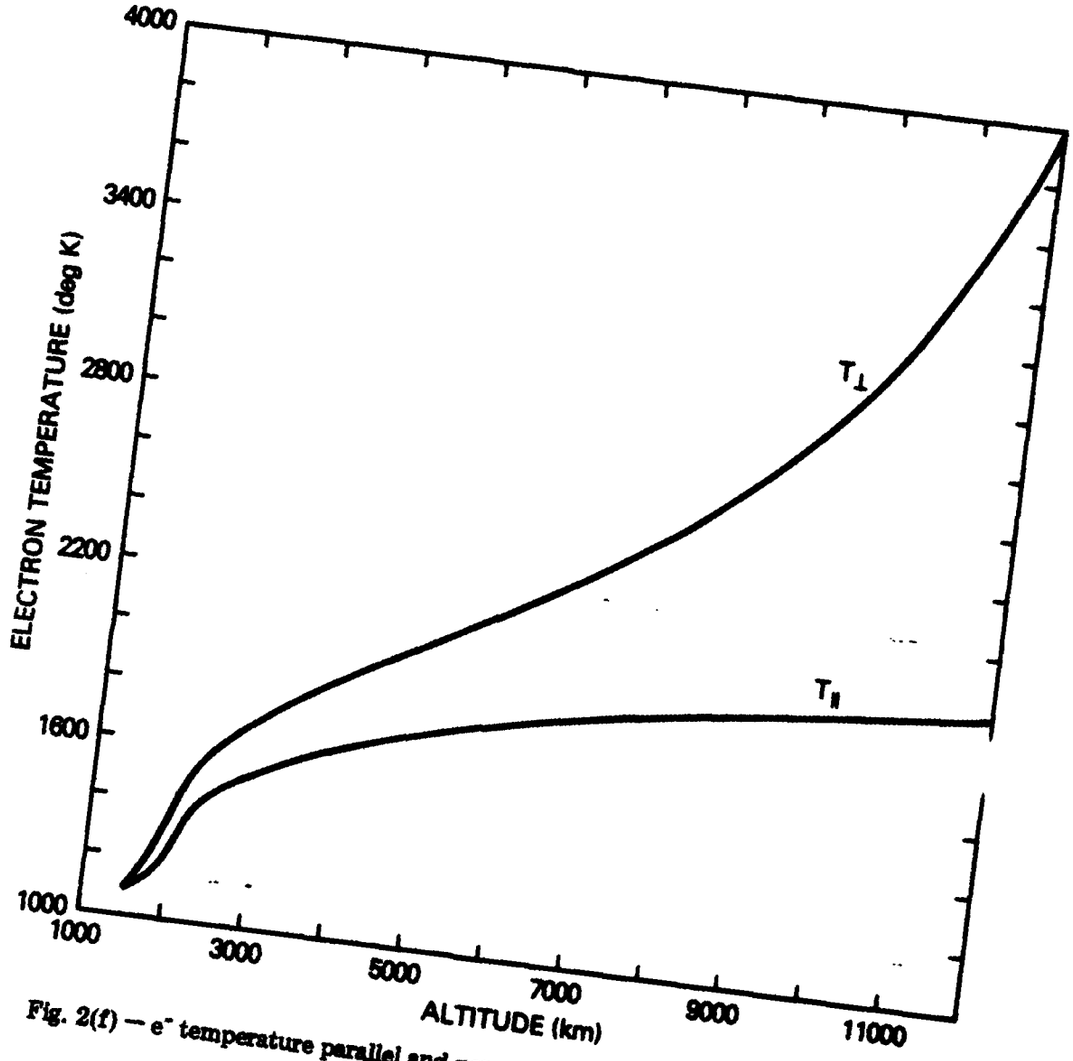

Fig. 2(f) — e^- temperature parallel and perpendicular to the geomagnetic field

Appendix 1

$$\frac{\delta n_b}{\delta t} = 0 \tag{1}$$

$$\frac{\delta v_b}{\delta t} = \sum_a \nu_{ba} (v_a - v_b)(1 + \Phi_{ba}) \tag{2}$$

$$k \frac{\delta t_{b\parallel}}{\delta t} = \sum_a \frac{m_b \nu_{ba}}{(m_b + m_a)} \left\{ \frac{6}{5} kT_{a\parallel} - \left[2 + \frac{4m_a}{5m_b} \right] kT_{b\parallel} \right.$$

$$\left. + \frac{4}{5} KT_{a\perp} + \frac{4m_a}{5m_b} kT_{b\perp} + \left[2kT_a + \left(4 + 6 \frac{m_a}{m_b} \right) kT_b \right] \Phi_{ba} \right\} \tag{3}$$

$$k \frac{\delta T_{b\perp}}{\delta t} = \sum_a \frac{m_b \nu_{ba}}{(m_b + m_a)} \left[3kT_a - 3kT_b + m_a (v_a - v_b)^2 (1 + \Phi_{ba}) \right] - \frac{k}{2} \frac{\delta T_{b\parallel}}{\delta t} \tag{4}$$

$$\frac{\delta q_{b\parallel}}{\delta t} = - \nu_b q_{b\parallel} \tag{5}$$

$$\frac{\delta q_{b\perp}}{\delta t} = - \nu_b q_{b\perp} \tag{6}$$

Each sum includes all charged particles species in the simulation. the velocity - corrected Coulomb collision frequency ν_{ba} is given by

$$\nu_{ba} = \frac{n_a (32\pi)^{1/2} e_b^2 e_a^2 (m_b + m_a) \ln A \exp(-x_{ba}^2)}{3 m_b^2 m_a \alpha_{ba}^3} \qquad (7)$$

(ln A is the Coulomb logarithm), and

$$T_b = \frac{1}{3} T_{b\parallel} + \frac{2}{3} T_{b\perp}$$

$$\alpha_{ba}^2 = \frac{2kT_b}{m_b} + \frac{2kT_a}{m_a}$$

$$x_{ba}^2 = \frac{(v_b - v_a)^2}{\alpha_{ba}^2}$$

$$\Phi_{ba} = \frac{2}{5} x_{ba}^2 + \frac{4}{35} x_{ba} + \frac{8}{315} x_{ba}$$

Acknowledgments

We would like to thank Dr. R.W. Schunk, Dr. S.J. Marsh and Dr. I. Haber for useful discussions. This work is supported by the Office of Naval Research and the National Aeronautics and Space Administration.

References

Banks, P.M. and T.E. Holzer, The Polar Wind, J. Geophys. Res., 73, 6846-6854, 1968.

Banks, P.M. and T.E. Holzer, High-Latitude Plasma Transport: The Polar Wind, J.Geophys. Res., 74 6317-6332, 1969.

Barakat, A.R., and R.W. Schunk, Transport Equations for Multicomponent Anisotropic Space Plasmas, Plasma Physics, 24, 389-418, 1982.

Burgers, J.M., Flow Equations for Composite Gases, Academic Press, New York, 1969

Holzer, T.E., J.A. Fedder, and P.M. Banks, A Comparison of Kinetic and Hydrodynamic Models of an Expandig Ion-Exosphere, J.Geophys. Res., 76 2453-2468, 1971.

Lemaire, J., and M. Scherer, Kinetic Models of the Solar and Polar Winds, Rev. Geophys. Space Phys., 11, 427-468, 1973.

Mitchell, H.G., Jr., and P.J. Palmadesso, A Dynamic Model for the Auroral Field Line Plasma in the Presence of Field-Aligned Current. J. Geophys. Res., 88, 2131, 1983.

Nagai, T., J.H. Waite, J.L. Green, C.R. Chappell, R.C. Olsen, and R.H. Comfort, First Measurements of Supersonic Polar Wind in the Polar Magnetosphere, Res. Lett., 11, 669-672, 1984.

Schunk, R.W., Mathematical Structure of Transport Equations for Multispecies Flows, Rev. Geophys. Space Phys., 15, 429-445, 1977

Schunk, R.W. and D.S. Watkins, Electron Temperature Anisotropy in the Polar Wind, J.Geophys. Res., 86, 91-102, 1981.

Schunk, R.W. and D.S. Watkins, Proton Temperature Anisotropy in the Ploar Wind, J.Geophys. Res., 87 171-180, 1982.

Shampine, L.F. and C.W. Gear, A User's View of Solving Stiff Ordinary Differential Equations, SIAM Rev., 21, 1-17, 1979.

Watkins, D.S. Efficient initialization of Stiff Systems with One Unknown Initial Condition, SIAM J. Numer. Anal., 18, 794-800, 1981.

DISTRIBUTION LIST

Director
Naval Research Laboratory
Washington, D.C. 20375
ATTN: Code 4700 (26 Copies)
Code 4701
Code 4780 (50 copies)
Code 4706 (P. Rodriguez)
Code 2628 (22 Copies)

University of Alaska
Geophysical Institute
Fairbanks, Alaska 99701
ATTN: Library
S. Akasofu
J. Kan
J. Roederer
L. Lee

University of Arizona
Dept. of Planetary Sciences
Tucson, Arizona 85721
ATTN: J.R. Jokipii

University of California, S.D.
LaJolla, California 92037
(Physics Dept.):
ATTN: J.A. Fejer
T. O'Neil
J. Winfrey
Library
J. Malmberg
(Dept. of Applied Sciences):
ATTN: H. Booker

University of California
Los Angeles, California 90024
(Physic Dept.):
ATTN: J.M. Dawson
B. Fried
J.G. Moralles
W. Gekelman
R. Stenzel
Y. Lee
A. Wong
F. Chen
M. Ashour-Abdalla
Library
J.M. Cornwall

(Institute of Geophysics and
Planetary Physics):
ATTN: Library
C. Kennel
F. Coroniti

Columbia University
New York, New York 10027
ATTN: R. Taussig
R.A. Gross

University of California
Berkeley, California 94720
(Space Sciences Laboratory):
ATTN: Library
M. Hudson
(Physics Dept.):
ATTN: Library
A. Kaufman
C. McKee
(Electrical Engineering Dept.):
ATTN: C.K. Birdsall

University of California
Physics Department
Irvine, California 92664
ATTN: Library
G. Benford
N. Rostoker
C. Robertson
N. Rynn

California Institute of Technology
Pasadena, California 91109
ATTN: R. Gould
L. Davis, Jr.
P. Coleman

University of Chicago
Enrico Fermi Institute
Chicago, Illinois 60637
ATTN: E.N. Parker
I. Lerche
Library

Thayer School of Engineering
Dartmouth College
Hanover, NH 03755
ATTN: Bengt U.O. Sonnerup

University of Colorado
Dept. of Astro-Geophysics
Boulder, Colorado 80302
ATTN: M. Goldman
Library

Cornell University
School of Applied and Engineering Physics
College of Engineering
Ithaca, New York 14853
ATTN: Library
R. Sudan
B. Kusse
H. Fleischmann
C. Wharton
F. Morse
R. Lovelace

Harvard University
Cambridge, Massachusetts 02138
ATTN: Harvard College Observatory
(Library)
G.S. Vaina
M. Rosenberg

Harvard University
Center for Astrophysics
60 Garden Street
Cambridge, Massachusetts 02138
ATTN: G.B. Field

University of Iowa
Iowa City, Iowa 52240
ATTN: C.K. Goertz
D. Gurnett
G. Knorr
D. Nicholson

University of Houston
Houston, Texas 77004
ATTN: Library

University of Maryland
Physics Dept.
College Park, Maryland 20742
ATTN: K. Papadopoulos
H. Rowland
C. Wu

University of Michigan
Ann Arbor, Michigan 48140
ATTN: E. Fontheim

University of Minnesota
School of Physics
Minneapolis, Minnesota 55455
ATTN: Library
J.R. Winckler
P. Kellogg

M.I.T.
Cambridge, Massachusetts 02139
ATTN: Library
(Physics Dept.):
ATTN: B. Coppi
V. George
G. Bekefi
T. Chang
T. Dupree
R. Davidson
(Elect. Engineering Dept.):
ATTN: R. Parker
A. Bers
L. Smullin
(R.L.E.):
ATTN: Library
(Space Science):
ATTN: Reading Room

Princeton University
Princeton, New Jersey 08540
Attn: Physics Library
Plasma Physics Lab.
Library
C. Oberman
F. Perkins
T.K. Chu
H. Okuda
V. Aranasalan
H. Hendel
R. White
R. Kurlsrud
H. Furth
S. Yoshikawa
P. Rutherford

Rice University
Houston, Texas 77001
Attn: Space Science Library
R. Wolf

University of Rochester
Rochester, New York 14627
ATTN: A. Simon

Stanford University
Institute for Plasma Research
Stanford, California 94305
ATTN: Library

Stevens Institute of Technology
Hoboken, New Jersey 07030
ATTN: B. Rosen
G. Schmidt
M. Seidl

University of Texas
Austin, Texas 78712
ATTN: W. Drummond
V. Wong
D. Ross
W. Horton
D. Choi
R. Richardson
G. Leifeste

College of William and Mary
Williamsburg, Virginia 23185
Attn: F. Crownfield

Lawrence Livermore Laboratory
University of California
Livermore, California 94551
ATTN: Library
B. Kruer
J. Thomson
J. Nucholls
J. DeGroot
L. Wood
J. Emmett
B. Lasinsky
B. Langdon
R. Briggs
D. Pearlstein

Los Alamos National Laboratory
P.O. Box 1663
Los Alamos, New Mexico 87545
ATTN: Library
D. Forslund
J. Kindel
B. Bezzerides
H. Dreicer
J. Ingraham
R. Boyer
C. Nielson
E. Lindman
L. Thode

N.O.A.A.
325 Broadway S.
Boulder, Colorado 80302
ATTN: J. Weinstock
Thomas Moore (SEL, R-43)
W. Bernstein
D. Williams

Sandia Laboratories
Albuquerque, New Mexico 87115
ATTN: A. Toepfer
G. Yeonas
D. VanDevender
J. Freeman
T. Wright

Bell Laboratories
Murray Hill, New Jersey 07974
ATTN: A. Hasegawa

Lockheed Research Laboratory
Palo Alto, California 94304
ATTN: M. Walt
J. Cladis
J. Siambis

Physics International Co.
2400 Merced Street
San Leandro, California 94577
ATTN: J. Benford
S. Putnam
S. Stalings
T. Young

Science Applications, Inc.
Lab. of Applied Plasma Studeis
P.O. Box 2351
LaJolla, California 92037
ATTN: L. Linson
J. McBride

NASA/Goddard Space Flight Center
Greenbelt, Maryland 20771
ATTN: M. Goldstein
T. Northrop
T. Birmingham

NASA/Goddard Space Flight Center
Greenbelt, MD 20771
ATTN: A. Figuero Vinas
Code 692

TRW Space and Technology Group
Space Science Dept.
Building R-1, Room 1170
One Space Park
Redondo Beach, California 90278
ATTN: R. Fredericks
W.L. Taylor

National Science Foundation
Atmospheric Research Section (ST)
Washington, D.C. 20550
ATTN: D. Peacock

Goddard Space Flight Center
Code 961
Greenbelt, Maryland 20771
ATTN: Robert F. Benson

NASA Headquarters
Code EE-8
Washington, D.C. 20546
ATTN: Dr. E. Schmerling
Dr. J. Lynch
Dr. D. Butler

Klumpar, David
Center for Space Sciences
P.O. Box 688
University of Texas
Richardson, Texas 75080

Leung, Philip
Dept. of Physics
University of California
405 Hilgard Avenue
Los Angeles, California 90024

Lysak, Robert
School of Physics and Astronomy
University of Minnesota
Minneapolis, MN 55455

Schulz, Michael
Aerospace Corp.
A6/2451, P.O. Box 92957
Los Angeles, California 90009

Shawhan, Stanley
Dept. of Physics & Astronomy
University of Iowa
Iowa City, Iowa 52242

Temerin, Michael
Space Science Lab.
University of California
Berkeley, California 94720

Vlahos, Loukas
Dept. of Physics
University of Maryland
College Park, Maryland 20742

Matthews, David
IPST
University of Maryland
College Park, Maryland 20742

Schunk, Robert W.
Utah State University
Dept. of Physics
Logan, Utah 84322

Director,
Department of Energy
ER20:GTN, High Energy &
Nuclear Physics
Washington, D.C. 20545
ATTN: Dr. Terry Godlove

Director,
Department of Energy
Office of Inertial Fusion
Washington, D.C. 20545
ATTN: Dr. Richard Schriever

Director
Defense Nuclear Agency
Washington, D.C. 20305
ATTN: Dr. Leon Wittwer
Dr. P. Crowley
Dr. Carl Fitz

Director of Research
U.S. Naval Academy
Annapolis, MD 21402 (2 copies)

END

FILMED

9-85

DTIC